



UNIVERSITY OF LEEDS

This is a repository copy of *Morphology of order-disorder structures in rapidly solidified L12 intermetallics*.

White Rose Research Online URL for this paper:
<http://eprints.whiterose.ac.uk/109299/>

Version: Accepted Version

Proceedings Paper:

Haque, N orcid.org/0000-0002-0271-9209, Cochrane, RF and Mullis, AM orcid.org/0000-0002-5215-9959 (2017) Morphology of order-disorder structures in rapidly solidified L12 intermetallics. In: TMS 2017 Conference Proceedings (Frontiers in Solidification Science). TMS 2017 Spring Meeting, 26 Feb - 02 Mar 2017, San Diego, US. Springer International Publishing , pp. 729-736. ISBN 978-3-319-51493-2

https://doi.org/10.1007/978-3-319-51493-2_70

© The Minerals, Metals & Materials Society 2017. This is an author produced version of a paper published in TMS 2017 146th Annual Meeting & Exhibition Supplemental Proceedings. Uploaded in accordance with the publisher's self-archiving policy.

Reuse

Items deposited in White Rose Research Online are protected by copyright, with all rights reserved unless indicated otherwise. They may be downloaded and/or printed for private study, or other acts as permitted by national copyright laws. The publisher or other rights holders may allow further reproduction and re-use of the full text version. This is indicated by the licence information on the White Rose Research Online record for the item.

Takedown

If you consider content in White Rose Research Online to be in breach of UK law, please notify us by emailing eprints@whiterose.ac.uk including the URL of the record and the reason for the withdrawal request.



eprints@whiterose.ac.uk
<https://eprints.whiterose.ac.uk/>

Morphology of order-disorder structures in rapidly solidified L12 intermetallics

Nafisul Haque^{1, a*}, Robert F Cochrane^{1, b} and Andrew M Mullis^{1, c}

¹Institute for Materials Research, University of Leeds, Leeds LS2 9JT, UK.

^apmnh@leeds.ac.uk, ^bR.F.Cochrane@leeds.ac.uk, ^cA.M.Mullis@leeds.ac.uk

Keywords: Intermetallics; Rapid Solidification; Disorder Trapping; Spherulites.

Abstract

Utilization of intermetallics in high temperature applications is limited due to their poor room temperature ductility. One route to overcoming this is disorder trapping (and subsequent anti-phase domain formation) during rapid solidification, motivating the study of disorder trapping in intermetallics. The single-phase, L1₂ intermetallic β -Ni₃Ge has been rapidly solidified via drop-tube processing. At low cooling rates (850 – 500 μm diameter particles, 700 – 2800 K s⁻¹) the dominant solidification morphology, revealed after etching, is that of isolated spherulites in an otherwise featureless matrix. Selected area diffraction analysis in the TEM reveals the spherulites to be partially disordered β -Ni₃Ge, whilst the featureless matrix is the fully ordered variant of the same compound. Dark-field TEM imaging has confirmed that the spherulites grow as radially emanating fingers of the ordered phase, with disordered material in the space between the fingers.

Introduction

Intermetallic compounds are characterised by strong internal order and mixed covalent/ionic and metallic bonding, which gives rise to mechanical behaviour intermediate between ceramics and metals [1]. They have a range of potential applications as high temperature structural materials due to good chemical stability and high hardness at elevated temperatures. Conversely, poor room temperature ductility limits formability. Low temperature ductility can be increased by rapid solidification processing, wherein a reduction of the degree of order and the formation of antiphase domains increases ductility [2-4]. Moreover, the high temperature properties can be restored by annealing to restore chemical ordering [2].

In this article we present an analysis of the rapid solidification of the single phase, congruently melting, intermetallic β -Ni₃Ge, a compound which at equilibrium orders at all temperatures below the liquidus. The main motivation for this is to study the solidification morphologies associated with disorder trapping at high growth rate without the associated complication of solute trapping. However, as the main solidification morphology observed are spherulites, a relatively uncom-

mon morphology in metals and intermetallics, we first present a review of the spherulite morphology and its previous occurrence in metallic systems.

The crystalline morphology termed spherulitic was first observed by Talbot in 1837 during the crystallisation of borax from phosphoric acid [5]. Spherulites are commonly observed in polymers and small molecule organic crystals, together with some minerals, volcanic rocks, inorganic crystals and a few pure elements (e.g. graphite, sulphur and selenium) [6]. Spherulites are only rarely observed in metals, sometimes as graphite formations in cast irons and otherwise as the result of devitrification of metallic glasses [6].

As mentioned above, spherulites are most common in polymers, particularly those of high molecular weight grown directly from the melt, where topological constraints restricting the reorientation of long chain molecules are encountered. The structure of such spherulites is of multiply branched crystalline arms separated by amorphous regions between the arms [6]. The formation of spherulites is most common in unoriented systems. Where a strong tendency for uniform molecular orientation exists, such as for growth in a strong, externally imposed temperature gradient, spherulite growth appears to be suppressed [7].

Spherulite growth is also observed in a number of metallic systems, particularly during the devitrification of amorphous metals. Chrissafis *et al.* [8] studied the crystallisation of Fe-Si-B metallic glass in the solid-state, observing the formation of Fe spherulites, the distribution of which was indicative of homogenous nucleation and isolated, diffusion controlled three dimensional growth in the amorphous matrix. Yano *et al.* [9] observed spherulite formation in $Zr_{50}Cu_{40}Al_{10}$ bulk metallic glass, annealed at 773 K, using TEM and positron annihilation lifetime measurements. Crystallisation proceeded by the formation of spherical agglomerates of radially developing crystalline grains, some 600 nm in diameter. Various other studies [9-12], looking at the crystallisation products of devitrification in binary and multicomponent metallic glasses, have made similar observations of spherulite structures. The results appear to be insensitive to heating rate, with heating rates as high as 10^3 K s^{-1} being found not to inhibit spherulite formation [13].

Although there is controversy in the literature as to the formation mechanism for spherulitic growth, a number of common requirements for their formation have been identified. One is a tendency towards non-crystallographic, small angle branching [14]. A second is a high viscosity in the medium being crystallised. The importance of this has been demonstrated unambiguously by Morse *et al.* [15, 16] who, in a study of the crystallisation behaviour of inorganic salts, identified around 70 salts that would crystallise in spherulitic form if grown in a gel, but not otherwise. It has been suggested that spherulite growth may be favoured in situations where translational diffusion may be significantly easier than rotational diffusion [17] and one can certainly imagine how this situation might arise during the crystallisation of long chain polymers, although it is less obvious how such a situation might arise in metals or other small molecular systems. Despite this, there is some evidence that similar conditions may exist in both organic [18] and metallic [19] undercooled glass forming liquids, with a decoupling of the translational

diffusion coefficient from the macroscopic viscosity and a decoupling of the translational and rotational diffusion coefficients. The propensity of metallic glass formers to form spherulites is also suggestive of the requirement for some level of structure in the non-crystalline precursor to be a prerequisite. This also appears to be true of other spherulite formers, such as pure elemental Se, which is reported to have a very peculiar molecular structure, intermediate between truly polymeric and simple molecular liquids [20].

According to the phase diagram of Nash and Nash [21], β -Ni₃Ge is a congruently melting compound with a melting point of 1405 K. It has a homogeneity range of 22.5 to 25 at. % Ge and crystallizes to the ordered fcc L1₂ structure. The system has previously been studied by Ahmed *et al.* [22] who, using a flux undercooling technique, observed a maximum undercooling of 362 K, wherein the corresponding growth velocity was measured at 3.55 m s⁻¹. In common with other researchers who have determined the velocity-undercooling curves for intermetallic compounds passing through the order-disorder transformation, Ahmed *et al.* observed a discontinuous break in the curve at the onset of fully disordered growth. This condition was observed for β -Ni₃Ge at an undercooling of 168 K and at a critical growth velocity, V_C , of 0.22 m s⁻¹. More recently Haque *et al.* [23] have observed a range of solidification structures in rapidly solidified Ni₃Ge including a dendritic to dendritic seaweed transition.

Experimental Methods

Elemental Ni and Ge were obtained from Alfa Aesar with purity of 99.99 % and 99.999%, metals basis, respectively. The alloy, of composition Ni-25 at. % Ge, was produced by arc-melting the elemental constituents together under a protective argon atmosphere, with the melting process being repeated 8 times to ensure uniform mixing of the final alloy. Following arc-melting the phase composition of the alloy ingot was checked using a PANalytical Xpert Pro X-ray diffractometer and drop-tube processing was only undertaken on samples that were confirmed as single phase β -Ni₃Ge.

The alloy sample, of approximately 9.5 g mass, was loaded into an alumina crucible which has three 300 μ m laser drilled holes in the base. Induction heating of a graphite subsector was used for melting the sample. Temperature determination was by means of an R-type thermocouple which sits inside the melt crucible, just above the level of the melt. When the temperature in the crucible attained 1480 K (75 K superheat) the melt was ejected by pressuring the crucible with \sim 400 kPa of N₂ gas. The resulting spray of particles solidify in-flight whilst falling the 6.5 m length of the tube, which is filled to 50 kPa with dry, oxygen free N₂ gas, and are collected at the base of the tube. Further details of the Leeds drop-tube and the likely cooling rates that can be thus achieved can be found in [24].

Following retrieval of the sample from the base of the drop-tube the powders were sieved into standard size fractions, with the size fractions, $> 850\mu\text{m}$ and $850 - 500 \mu\text{m}$ being selected for analysis here. Using the method given by [24] the mean post-recalcence cooling rate for these two size fractions is estimated at 700 K s^{-1} and 2800 K s^{-1} respectively.

The selected size fractions were subject to XRD analysis to ensure they remained single-phase and were then mounted in transopic resin and prepared for microstructural analysis. This involved grinding with SiC grinding media and then polishing with progressively finer grades of diamond paste, finishing with a $1 \mu\text{m}$ grade. $\beta\text{-Ni}_3\text{Ge}$ was found to be highly resistant to most chemical etchants normally used in metallography. The etchant used was the aggressive mix consisting equal parts of undiluted HF, HCl and HNO_3 . A Carl Zeiss EVO MA15 scanning electron microscope (SEM) was used to image the microstructure of the droplets revealed by etching while an Oxford Instrument X-Max Energy-Dispersive X-Ray (EDX) detector was used to check the chemical homogeneity of the samples. Selected area diffraction analysis and bright-field imaging was performed using a FEI Tecnai TF20 Transmission Electron Microscope (TEM), with samples, of approximately $10 \mu\text{m} \times 7 \mu\text{m}$ and between 55-70 nm in thickness, being cut using a FEI Nova 200 Nanolab focused ion beam (FIB).

Results & Discussion

Figure 1 (a) shows an SEM micrograph of a polished and etched sample from the $850\text{-}500 \mu\text{m}$ sieve fraction. Numerous spherulite like structures, typically with diameters of the order of $10\text{-}20 \mu\text{m}$, are evident in an otherwise featureless matrix. Such structures are very rare in metallic systems, although appear to be ubiquitous throughout the drop-tube powders in this size fraction. We note that, except for the spherulites, no other crystalline features are revealed in the sample by etching. XRD analysis (not shown) performed on the powder samples confirms that the material remain single phase $\beta\text{-Ni}_3\text{Ge}$ subsequent to drop-tube processing. The contrast between the spherulite and the surrounding matrix material appears not to be the result of compositional differences due to solute partitioning during solidification. The absence of solute partitioning is demonstrated in Figure 1(b) which shows an EDX line across the diameter of a spherulite as revealed by etching. From this it is clear that, to within the experimental error associated with the technique, there is little variation in composition between the structures revealed by etching and the surrounding featureless matrix. The contrast revealed by etching does not therefore appear to be related to differences in either phase (XRD) or chemical (EDX) composition.

In order to understand the origins of the spherulite morphology TEM imaging and Selected Area Diffraction (SAD) analysis has been performed. Figure 2(a) shows typical bright-field TEM image of an isolated spherulite. Figures 2(b & c)

show two selected area diffraction patterns obtained from the microstructure shown in Figure 2(a), taken (i) from the spherulites structure, and (ii) from the initial core of the spherulite. Both are consistent with an fcc cubic structure with the lattice parameters of β -Ni₃Ge. However, (b) also displays superlattice spots consistent with the ordered L₁₂ crystal structure of β -Ni₃Ge, as expected from the phase diagram, while (c) shows no such superlattice spots and thus appears to be the disordered A1 fcc structure. Beyond the spherulites, similar SAD pattern analysis (not shown) confirms that all of the featureless matrix material has the fully ordered L₁₂ crystal structure.

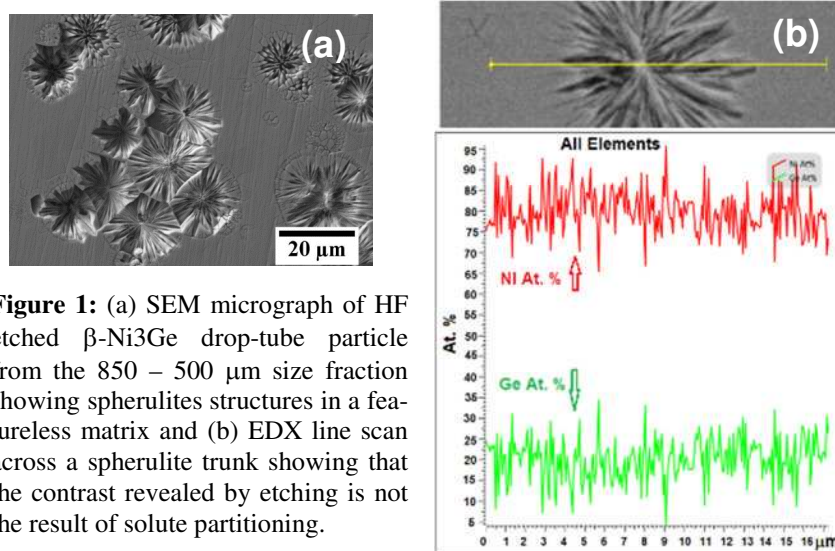


Figure 1: (a) SEM micrograph of HF etched β -Ni₃Ge drop-tube particle from the 850 – 500 μ m size fraction showing spherulites structures in a featureless matrix and (b) EDX line scan across a spherulite trunk showing that the contrast revealed by etching is not the result of solute partitioning.

Figure 2(d) shows a TEM dark-field image of a region within a spherulite obtained from one of the superlattice spots within the diffraction pattern. The spherulite appears to consist of fingers of material that are bright and are likely to therefore be of the ordered phase, with a dark, and therefore probably disordered material between the fingers. In common with many polymer spherulites the fingers within a spherulite are generally observed to be of uniform width and in order to achieve space filling whilst maintaining a constant width the fingers undergo non-crystallographic branching [25].

A number of amorphous metallic systems crystallize to a spherulitic morphology upon heating above the glass transition temperature. While in some respects crystallization from a metallic glass precursor is similar to crystallization from the melt, in other respects it is quite different. The main difference is that the viscosity of a glass is much higher than that of a melt and correspondingly, the atomic diffusivity is much lower in a glass, compared to a melt of the equivalent composition. Consequently, crystallization from a glass is often restricted to short range

diffusion. This in turn means that growth kinetics dominate over diffusion. An analogous situation may be considered to exist in the growth of β -Ni₃Ge from its parent melt. As the compound is congruently melting there is no requirement for long range solute transport by diffusion, which is consistent with EDX results. Moreover, Ahmed *et al.* noted the abnormally high viscosity of the Ni₃Ge melt, with undercooled droplets being able to be pulled into teardrop shapes. This characteristic may be indicative of structure in the liquid, in a fashion similar to that found glass forming melts.

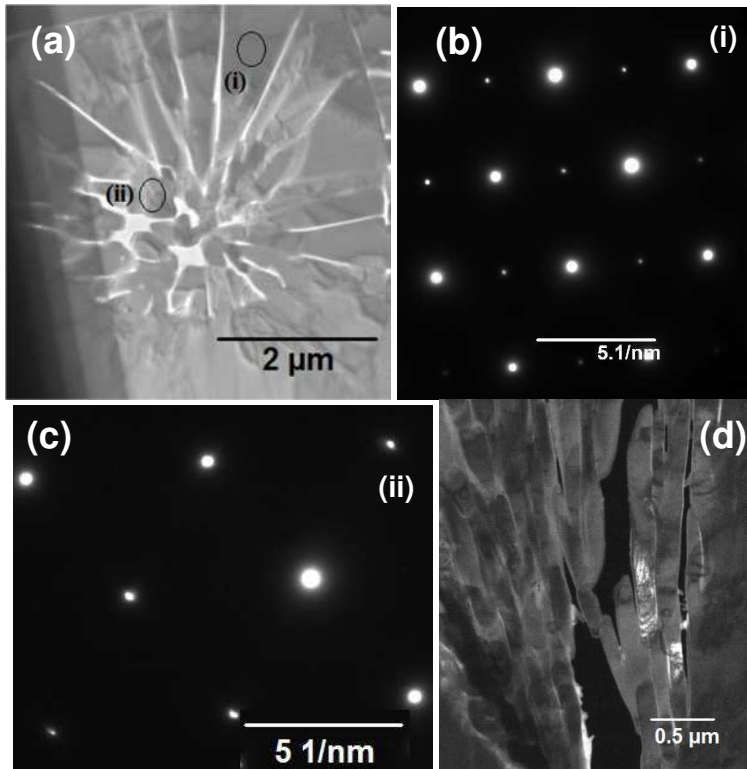


Figure 2: (a) TEM bright field image of a spherulite, (b) selected area diffraction patterns from regions (i) and (c) (ii) of the spherulite, and (d) TEM dark-field image of a region within a spherulite obtained from one of the superlattice spots within the diffraction pattern.

However, the morphological analogies between the spherulite structures observed here and those observed in polymers is significantly greater than previously reported for any form of metallic spherulite. These similarities include the growth of constant width fingers and space-filling by non-crystallographic branching. Moreover, the structure of the Ni₃Ge spherulites, with ordered fingers in a disordered matrix is analogous to the structure of polymer spherulites in which crystal-

line fingers are imbedded within an amorphous matrix. While the constant width fingers may be explained with recourse to a Mullins & Sekerka type instability, the non-crystallographic branching of an fcc metal is much more difficult to explain. The strong parallels between the spherulites observed here and those in polymers may suggest that some of the features of spherulites which have previously been attributed to the properties of their host polymer may in fact be inherent features of the spherulite morphology.

Acknowledgements

Nafisul Haque is thankful to the Higher Education Commission (HEC) Pakistan and NED University of Engineering & Technology Pakistan for financial support.

References

- [1] S. Murarka, *Metallization: Theory and practice for VLSI application*, (1993).
- [2] R. Cahn, P. Siemers, J. Geiger, P. Bardhan, "The order-disorder transformation in Ni_3Al and $\text{Ni}_3\text{Al-Fe}$ alloys—I. Determination of the transition temperatures and their relation to ductility", *Acta metallurgica*, 35 (1987), 2737-2751.
- [3] A. Inoue, H. Tomioka, T. Masumoto, "Microstructure and mechanical properties of rapidly quenched L11 alloys in Ni-Al-X systems", *Metallurgical Transactions A*, 14 (1983), 1367-1377.
- [4] H. Assadi, M. Barth, A. Greer, D.M. Herlach, "Microstructural development in undercooled and quenched Ni_3Al droplets", in: *Materials Science Forum*, *Trans Tech Publ*, 1996, pp. 37-44.
- [5] W.H.F. Talbot, *Phil. Trans. R. Soc. London*, London, 1837.
- [6] J. Magill, Review spherulites: "A personal perspective", *Journal of materials science*, 36 (2001), 3143-3164.
- [7] A. Keller, "The spherulitic structure of crystalline polymers. Part I. Investigations with the polarizing microscope", *Journal of Polymer Science*, 17 (1955), 291-308.
- [8] K. Chrissafis, M. Maragakis, K. Efthimiadis, E. Polychroniadis, "Detailed study of the crystallization behaviour of the metallic glass $\text{Fe}_{75}\text{-Si}_9\text{-B}_{16}$ ", *Journal of alloys and compounds*, 386 (2005), 165-173.
- [9] T. Yano, Y. Yorikado, Y. Akeno, F. Hori, Y. Yokoyama, A. Iwase, A. Inoue, T.J. Konno, "Relaxation and crystallization behavior of the $\text{Zr}_{50}\text{Cu}_{40}\text{Al}_{10}$ metallic glass", *Materials transactions*, 46 (2005), 2886-2892.
- [10] K. Ziewiec, "Kinetics of phase transformations in $\text{Ni}_{87}\text{P}_{13}$ alloy upon heating", *Journal of alloys and compounds*, 397 (2005), 207-210.

- [11] C. Xia, L. Xing, W.-Y. Long, Z.-Y. Li, Y. Li, "Calculation of crystallization start line for Zr48-Cu45-Al7 bulk metallic glass at a high heating and cooling rate", *Journal of Alloys and Compounds*, 484 (2009), 698-701.
- [12] J. Liu, H. Zhang, H. Fu, Z.-Q. Hu, X. Yuan, "In situ spherical B2 CuZr phase reinforced ZrCuNiAlNb bulk metallic glass matrix composite", *Journal of Materials Research*, 25 (2010), 1159-1163.
- [13] H. Sun, K. Flores, "Microstructural analysis of a laser-processed Zr-based bulk metallic glass", *Metallurgical and Materials Transactions A*, 41 (2010), 1752-1757.
- [14] H. Keith, F. Padden Jr, "A phenomenological theory of spherulitic crystallization", *Journal of Applied Physics*, 34 (1963), 2409-2421.
- [15] H.W. Morse, C.H. Warren, J.D.H. Donnay, "Artificial spherulites and related aggregates", *American Journal of Science*, (1932), 421-439.
- [16] H. Morse, J. Donnay, "Optics and structure of three-dimensional spherulites", *American Mineralogist*, 21 (1936), 391-427.
- [17] L. Gránásy, T. Pusztai, G. Tegze, J.A. Warren, J.F. Douglas, "Growth and form of spherulites", *Physical Review E*, 72 (2005), 011605.
- [18] S.F. Swallen, P.A. Bonvallet, R.J. McMahon, M. Ediger, "Self-diffusion of tris-naphthylbenzene near the glass transition temperature", *Physical review letters*, 90 (2003), 015901.
- [19] A. Masuhr, T. Waniuk, R. Busch, W. Johnson, "Time scales for viscous flow, atomic transport, and crystallization in the liquid and supercooled liquid states of $Zr_{41.2}Ti_{13.8}Cu_{12.5}Ni_{10.0}Be_{22.5}$ ", *Physical Review Letters*, 82 (1999), 2290.
- [20] J. Bisault, G. Ryschenkow, G. Faivre, "Spherulitic branching in the crystallization of liquid selenium", *Journal of crystal growth*, 110 (1991), 889-909.
- [21] A. Nash, P. Nash, *Binary Alloy Phase Diagrams*, in: US National Bureau of Standards Monograph Series 25, Elsevier, ASM, Ohio, 1976, pp. 35.
- [22] R. Ahmad, R. Cochrane, A. Mullis, "Disorder trapping during the solidification of β -Ni₃Ge from its deeply undercooled melt", *Journal of Materials Science*, 47 (2012), 2411-2420.
- [23] N. Haque, R.F. Cochrane, A.M. Mullis, "Rapid solidification morphologies in Ni₃Ge: Spherulites, dendrites and dense-branched fractal structures", *Intermetallics*, 76 (2016), 70-77.
- [24] O. Oloyede, T.D. Bigg, R.F. Cochrane, A.M. Mullis, "Microstructure evolution and mechanical properties of drop-tube processed, rapidly solidified grey cast iron", *Materials Science and Engineering: A*, 654 (2016), 143-150.
- [25] B. Crist, J.M. Schultz, "Polymer spherulites: A critical review", *Progress in Polymer Science*, 56 (2016), 1-63.